Available online at www.sciencedirect.com

SciVerse ScienceDirect

Ceramics International 38 (2012) 5807–5811

CERAMICS INTERNATIONAL

www.elsevier.com/locate/ceramint

Identification of Ti incorporation into β-SiAlON crystal structure through transmission electron microscopy techniques

Hilmi Yurdakul, Servet Turan *

Department of Materials Science and Engineering, Faculty of Engineering, Anadolu University, Eskisehir, TR 26480, Turkey

Received 4 March 2012; received in revised form 9 April 2012; accepted 9 April 2012
Available online 16 April 2012

Abstract

In this paper, we report the transmission electron microscopy (TEM) observations on the incorporation of Ti transition metal element into β-SiAlON crystal structure in a bulk β-SiAlON–TiN composite material. Considering our energy dispersive X-ray (EDX) and electron energy loss (EEL) spectroscopy results acquired by using nanometre-scale focused electron probe in scanning transmission electron microscopy (STEM) mode, the Ti-K characteristic X-ray lines and Ti-$L_{3,2}$ edges were detected in the chemical composition of the β-SiAlON grains. These results clearly reveal that Ti can enter into the β-SiAlON crystal structure. It is anticipated that this data will provide the new engineering insights on the production of transition metal element doped SiAlON-based materials for different applications.

Keywords: B. Electron microscopy; B. Spectroscopy; D. SiAlON; Ti

1. Introduction

β-SiAlON is currently considered as one of the most significant phase, especially enhancing the fracture toughness of the advanced SiAlON-based ceramics due to its unique self-propagating needle-like microstructure following sintering [1]. Recently, β-SiAlON has also been used as a host material for the rare-earth doped light emitting diodes (LEDs) [2–5], since two different type of channels along the *c* axis of its crystal structure accommodate the additional interstitial atoms [6]. The high resolution *Z* (atomic number)-contrast imaging [7] reveals the precise atomic positions of rare-earth dopants in β-SiAlON crystal structure [6,8]. More expressly, the interstitial cerium (Ce) [6] and europium (Eu) [8] atoms prefer to locate in the hexagonal-shaped channels, whereas the ytterbium (Yb) [6] atoms exist in a narrower interstitial site which is positioned between the two hexagonal channels. Also, as different from the existence of the rare-earth atoms in β-SiAlON, our previous analytical TEM study [9] interestingly demonstrated that transition metals, e.g. chromium (Cr) and iron (Fe), can enter into β-SiAlON crystal structure.

β-SiAlON–TiN composites characteristically show high thermal conductivity and fracture toughness thus providing an outstanding material for cutting tool applications that is capable of easily dissipating the heat and able to withstand the severe impacts at elevated operating temperatures [10–12]. Furthermore, they exhibit superior electrical conductivity character with respect to monolithic SiAlON-based materials [13]. This also easily enables the use of electrical discharge machining (EDM) on the β-SiAlON–TiN without any deterioration in its final properties whilst obtaining the complex shaped parts, e.g. glow plugs, heaters, igniters, etc. [14,15].

Despite the fact that several studies were carried out on the properties and production routes of β-SiAlON–TiN composites [10–15], very little is known about the detailed microstructure of these materials.

The goal of the current research is, therefore, to investigate the incorporation possibilities of Ti into β-SiAlON crystal structure in β-SiAlON–TiN composite by using various transmission electron microscopy (TEM) techniques.

2. Experimental

20% TiN containing SiAlON composites were produced with the addition of Si_3N_4, Al_2O_3 and Y_2O_3 by using gas pressure sintering technique under nitrogen atmosphere [12].

* Corresponding author. Tel.: +90 222 3213550x6356; fax: +90 222 3239501.
E-mail address: sturan@anadolu.edu.tr (S. Turan).

0272-8842/$36.00
http://dx.doi.org/10.1016/j.ceramint.2012.04.028

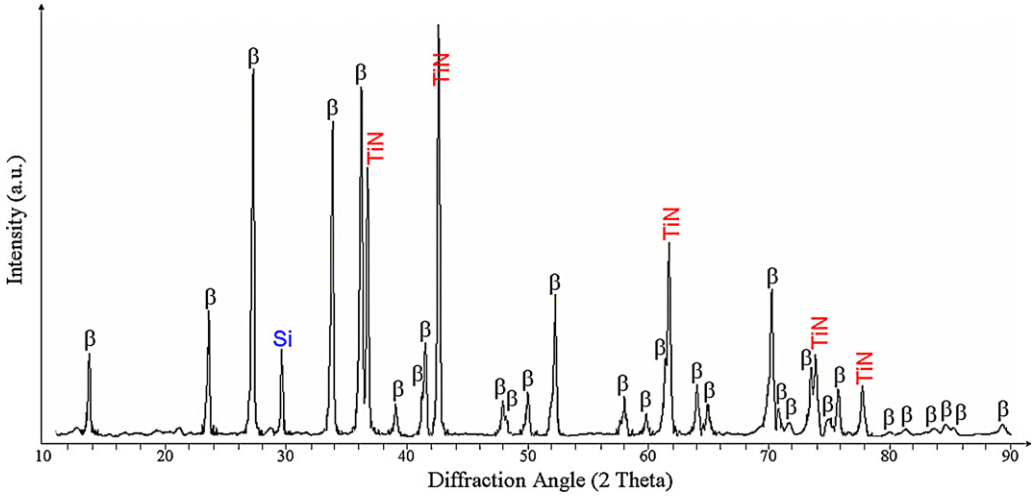

Fig. 1. The XRD pattern of β-SiAlON–TiN composite material (The metallic Si was used as internal standard).

Please also note that TiN and Si_3N_4 starting powders contain small amount of TiO_2 and SiO_2 as a surface oxide layer. The densities of sintered pellets were measured by Archimedes' principle. The phase identification in sintered sample was carried out using a powder X-ray diffraction (XRD) technique (Rigaku RINT-2000). For TEM investigations, the electron transparent specimen was prepared by mechanical polishing, followed by Ar-ion beam thinning and finally carbon coated (Leica Microsystems EM RES101) to minimize charging effects. Afterwards, the sample was characterised by using a field emission TEM (Jeol 2100F), operating at 200 kV equipped with an energy filter (Gatan Inc., GIF Tridiem), parallel electron energy loss spectrometer (EELS), a high angle annular dark field-scanning transmission electron microscope (HAADF-STEM) detector (Fishione) and an energy dispersive X-ray (EDX) spectrometer (Jeol JED-2300T). In EELS and EDX analyses, an electron spot with 1–2 nm in diameter was used. The backgrounds in EELS analysis was subtracted according to power-law [16]. In EELS analysis, the convergence and collection semi-angles were used as 9.2 and 15.7 mrad, respectively. The hard X-ray aperture was also inserted to reduce the X-rays emitted from the parts of microscope column and specimen holder. Furthermore, a corrector was used to avoid drift during the EDX analysis.

3. Results and discussion

Density measurements showed that sintered pellets were almost fully dense (99.5%). Considering the XRD data shown in Fig. 1, the peaks were indexed as β-SiAlON and TiN (Osbornite) phases. In addition, no crystalline intergranular secondary phases were detected from the XRD pattern (Fig. 1).

The bright field (BF) TEM image in Fig. 2a shows the general microstructure of the material. Here, the most of β-SiAlON grains constituting the matrix phase were observed as grey contrast, whilst the round-shaped TiN grains were seen as black colour. In Fig. 2b, a hexagonal-shaped β-SiAlON grain oriented along the [0 0 0 1] low index zone axis was seen as dark contrast with respect to other phases in microstructure due to diffraction condition. Also, looking at *Z*-contrast STEM image in Fig. 3, this highlighted β-SiAlON grain can be clearly discerned surrounded by TiN and sintering additive-rich intergranular secondary phases with white contrast in the image as a result of enhanced electron-scattering coming from the high atomic numbers of Ti (*Z*: 22) and Y (*Z*: 39) elements. Additionally, the selected area electron diffraction (SAED) pattern recorded from the same grain (Fig. 4) showed that this grain was β-SiAlON oriented parallel to [0 0 0 1] low index zone axis. This SAED pattern was entirely consistent with the simulated kinematical SAED pattern obtained from the β-SiAlON phase along the [0 0 0 1] low index zone axis [9]. Taking into account high resolution (HR) TEM image in Fig. 5 that acquired from the interface highlighted with "1" in Fig. 2b, the triple junction phase adjacent to [0 0 0 1] β-SiAlON grain on the right is amorphous. This result also confirms the XRD analysis (Fig. 1) that there is no secondary crystalline phase existing in the material.

Considering the STEM-EDX analysis given in Fig. 6 that collected from the same [0 0 0 1] β-SiAlON grain shown in Figs. 2b and 3, it was found that the grain was containing the constituent elements of β-SiAlON, i.e. Si, Al, O and N. On the other hand, more surprisingly, an extra explicit characteristic X-ray line at approximately 4.5 keV corresponding to Ti-K was detected in the β-SiAlON grain. To confirm the novelty of this finding, a number of STEM-EDX analyses were also carried out from the different β-SiAlON grains and results are presented in Table 1. Here, all the analysed β-SiAlON grains were determined to contain Ti element. Thus, the average composition of Ti bearing β-SiAlON grains was calculated as $Ti_{0.40}Si_{50.67}Al_{2.67}O_{9.51}N_{36.75}$ (at.%) by using standardless Cliff–Lorimer quantification method [17].

Nevertheless, to strengthen our EDX results shown in Fig. 6 and Table 1, EELS analyses were also performed on the same [0 0 0 1] β-SiAlON grain and TiN phase that used as an internal standard to observe the positions of Ti-$L_{3,2}$ edges and comparatively indicated in Fig. 7. In view of the EEL spectrum in Fig. 7, the Ti-$L_{3,2}$ edges were clearly seen together with the N-K and O-K edges, which revealed that Ti

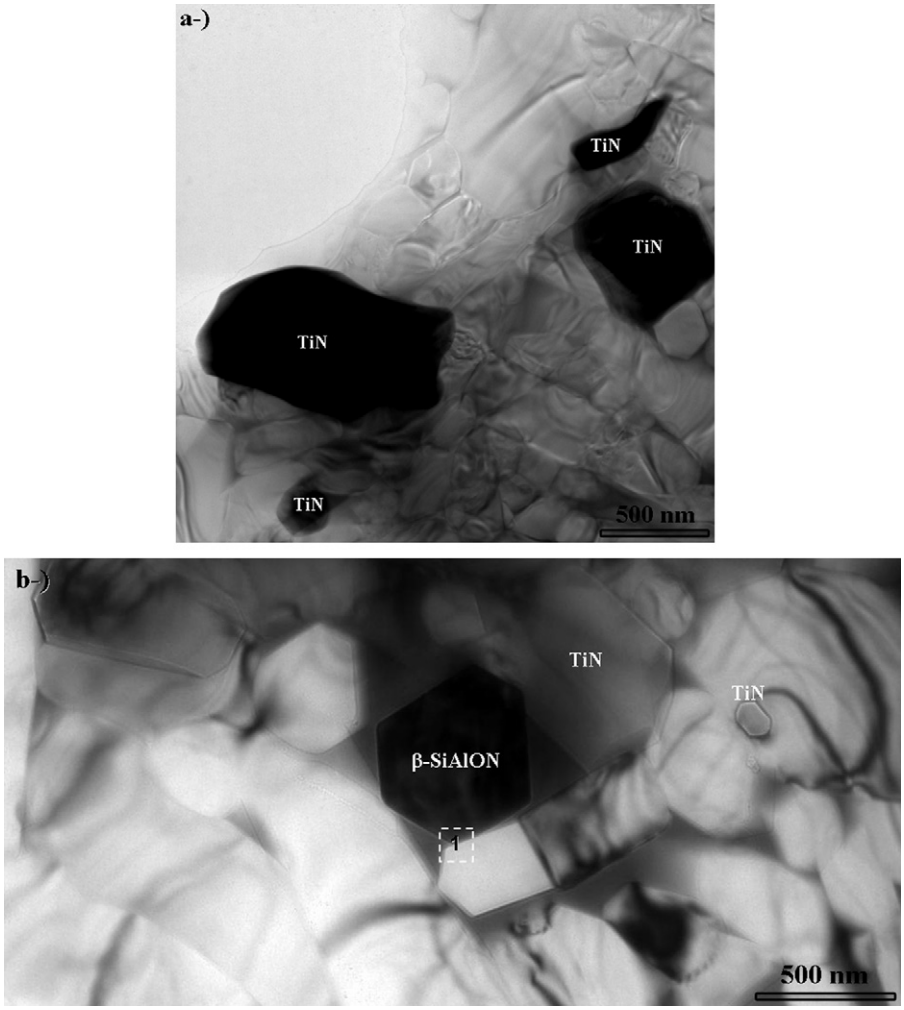

Fig. 2. TEM-BF images showing the (a) general microstructure of β-SiAlON–TiN composite material and (b) a hexagonal-shaped β-SiAlON grain oriented along the [0 0 0 1] low index zone axis.

existed in β-SiAlON grain. Furthermore, when Ti-$L_{3,2}$ edges in β-SiAlON was compared with internal reference EEL spectrum acquired from TiN phase in Fig. 7, it was observed that their edge positions shifted slightly forward, and edge shapes seemed not to be entirely similar to internal reference EEL spectrum of TiN. These chemical differences in Ti-$L_{3,2}$ edges provide further evidence that Ti is not coming from

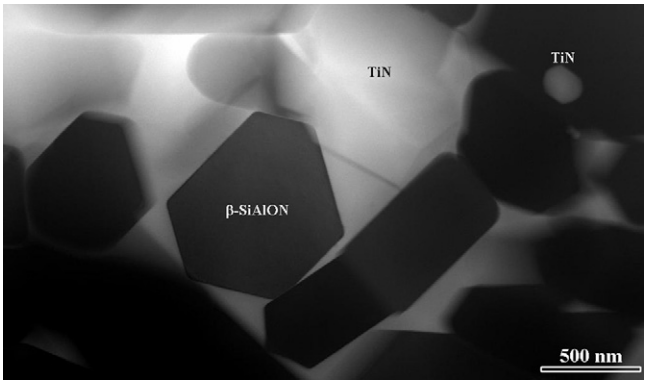

Fig. 3. *Z*-contrast STEM image of β-SiAlON–TiN composite material.

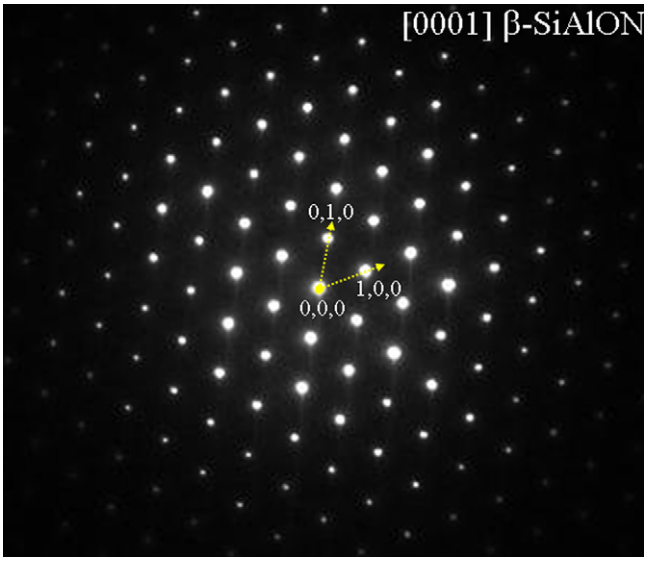

Fig. 4. SAED pattern acquired from the [0 0 0 1] low index zone axis of hexagonal-shaped β-SiAlON grain highlighted in Figs. 2b and 3.

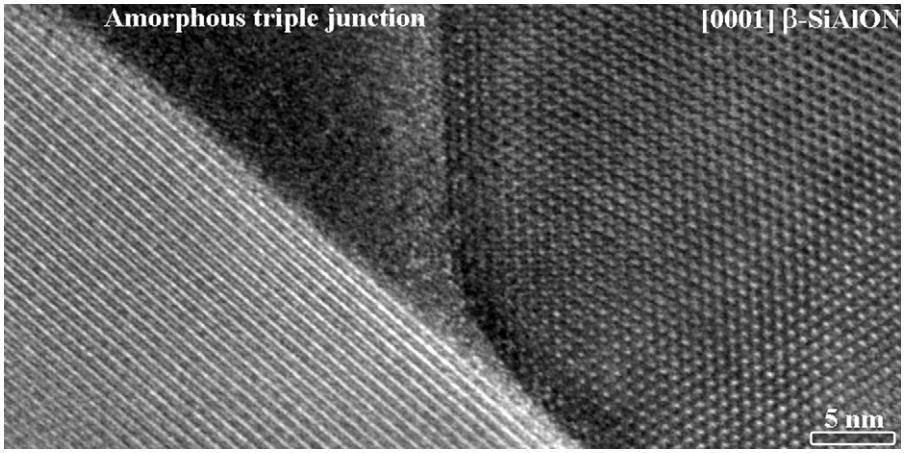

Fig. 5. HRTEM image obtained from the interface marked with ''1'' in Fig. 2b.

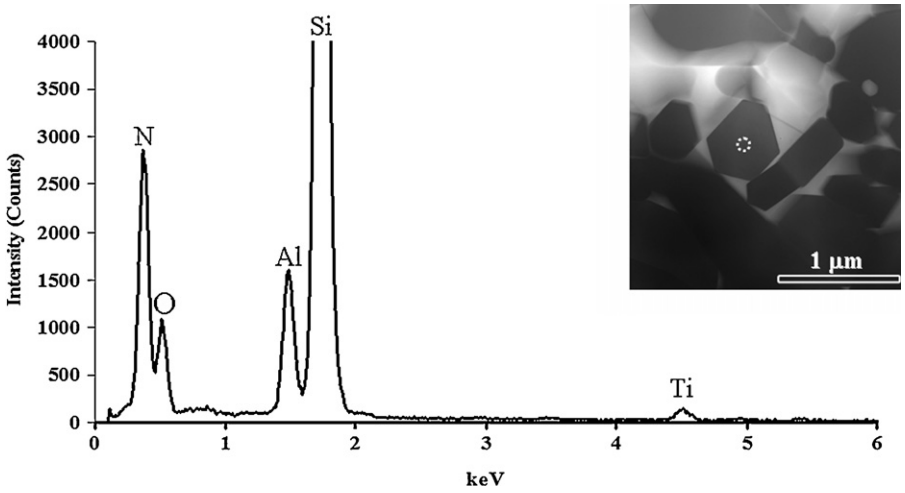

Fig. 6. EDX spectrum collected from the β-SiAlON grain in STEM mode (the white dotted circle on the inset *Z*-contrast STEM image shows where electron probe was focused during EDX analysis).

other sources but from the Ti incorporated into β-SiAlON crystal structure. At this point, we clearly state that Ti can enter into the β-SiAlON crystal structure.

In the light of experimental results presented, we think that the similarities in ionic radius of Si, Al and Ti elements are key factor for the understanding of how the Ti can enter into β-SiAlON crystal structure. The ionic radii of Si^{4+} and Al^{3+} are respectively 40 pm and 53 pm in four-fold coordination [18] since they exist in the $(Si,Al)(O,N)_4$ tetrahedrons in the β-SiAlON crystal structure [19]. Also, the ionic radius of Ti^{4+} is 56 pm in four-fold coordination [18]. Based on the ionic radii comparison, it can be deduced that the incorporation of Ti into β-SiAlON crystal structure is possible with substitution mechanism in the $(Si,Al)(O,N)_4$ tetrahedrons. In fact, the observation of Ti^{4+} substitution in SiN_xO_{4-x} and AlN_xO_{4-x} tetrahedrons strongly supports this prediction [20]. Additionally, this view was also discussed in a theoretical study [21] and explained that the incorporation of 3d-metal impurities such as

Table 1
The quantitative STEM-EDX analysis of β-SiAlON grains.

β-SiAlON	Elements (at.%)					Composition
	Ti	Si	Al	O	N	
Grain-1	0.36	51.24	5.01	9.94	33.45	$Ti_{0.36}Si_{51.24}Al_{5.01}O_{9.94}N_{33.45}$
Grain-2	0.48	50.21	1.58	8.53	39.20	$Ti_{0.48}Si_{50.21}Al_{1.58}O_{8.53}N_{39.20}$
Grain-3	0.51	50.51	2.76	8.22	38.00	$Ti_{0.51}Si_{50.51}Al_{2.76}O_{8.22}N_{38.00}$
Grain-4	0.36	50.22	2.12	10.26	37.04	$Ti_{0.36}Si_{50.22}Al_{2.12}O_{10.26}N_{37.04}$
Grain-5	0.31	51.16	1.88	10.62	36.03	$Ti_{0.31}Si_{51.16}Al_{1.88}O_{10.62}N_{36.03}$
Average	0.40 ± 0.09	50.67 ± 0.50	2.67 ± 1.38	9.51 ± 1.07	36.75 ± 2.18	$Ti_{0.40}Si_{50.67}Al_{2.67}O_{9.51}N_{36.75}$

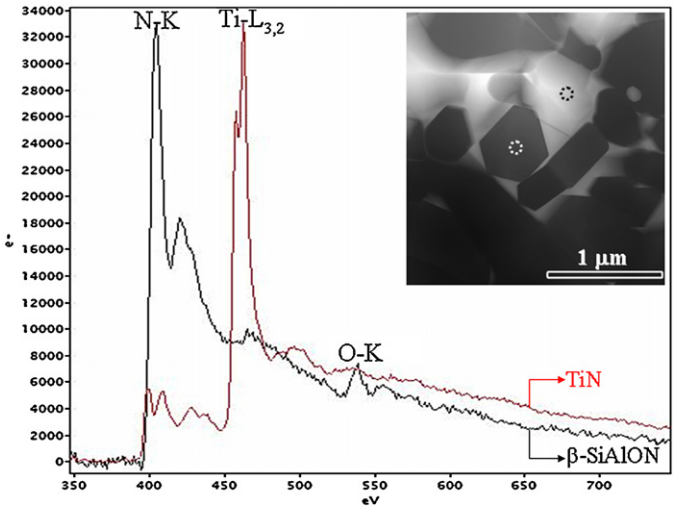

Fig. 7. EEL spectra recorded from the β-SiAlON and TiN grains in STEM mode (the white and black dotted circles on the inset *Z*-contrast STEM image show where electron probe was focused during EELS analysis).

Ti, Fe, and Cr could lead to a cation substitution mechanism in silicon oxynitride (Si_2N_2O) structure [21]. Furthermore, another theoretical study performed using first principles molecular orbital calculations expressed that the 3d-transition metal elements between Ti and Ni in the case of their formal 4+ oxidation state could constitute a solid solution in β-Si_3N_4 crystal structure [22]. Moreover, a study mentioned about a solid solution possibility of substituted Ti ion in the β-Si_3N_4 crystal lattice without an evidence of TEM results [23]. Therefore, Ti within the β-SiAlON phase observed in this study can enter the crystal structure through a substitution mechanism in Si(Al) sites of basic $(Si,Al)(O,N)_4$ tetrahedrons.

4. Conclusions

Here, we showed the TEM observations on the incorporation of Ti transition metal element into β-SiAlON crystal structure in β-SiAlON–TiN composite material. Based on our EDX and EEL spectroscopy results acquired in STEM mode, the Ti-K characteristic X-ray lines and Ti-$L_{3,2}$ edges were detected in the chemical composition of the β-SiAlON grains. These TEM findings clearly demonstrate that Ti enter into the β-SiAlON crystal structure. According to ionic radii comparisons and theoretical calculations, it can be concluded that Ti replaces Si and/or Al at substitutional positions. However, to determine exactly where Ti atoms are located in the β-SiAlON crystal structure, the atomic-resolved *Z*-contrast STEM imaging studies should be carried out. We anticipate that this data will provide the new engineering insights on the production of transition metal element doped SiAlON-based materials for different applications similar to rare-earth incorporated β-SiAlON materials for white light emitting diodes (LEDs).

Acknowledgement

The authors wish to express their gratitude to Dr. Orkun Tunckan for TEM sample preparation.

References

[1] S. Hampshire, Silicon nitride ceramics – review of structure, processing and properties, Journal of Achievements in Materials and Manufacturing Engineering 24 (2007) 43–50.
[2] N. Hirosaki, R.J. Xie, K. Kimoto, T. Sekiguchi, Y. Yamamoto, T. Suehiro, M. Mitomo, Characterization and properties of green-emitting β-SiAlON:Eu^{2+} powder phosphors for white light-emitting diodes, Applied Physics Letters 86 (2005) 211905.
[3] L.H. Liu, R.J. Xie, N. Hirosaki, T. Takeda, C.N. Zhang, J.G. Li, X.D. Sun, Optical properties of blue-emitting $Ce_xSi_{6-z}Al_{z-x}O_{z+1.5x}N_{8-z-x}$ for white light-emitting diodes, Journal of the Electrochemical Society 157 (2010) H50–H54.
[4] L. Liu, R.J. Xie, N. Hirosaki, T. Takeda, C.N. Zhang, J. Li, X. Sun, Photoluminescence properties of β-SiAlON:Yb^{2+}, a novel green-emitting phosphor for white light-emitting diodes, Science and Technology of Advanced Materials 12 (2011) 034404.
[5] T.C. Liu, B.M. Cheng, S.F. Hu, R.S. Liu, Highly stable red oxynitride β-SiAlON:Pr^{3+} phosphor for light-emitting diodes, Chemistry of Materials 23 (2011) 3698–3705.
[6] H. Yurdakul, J.C. Idrobo, S.J. Pennycook, S. Turan, Towards atomic scale engineering of rare-earth-doped SiAlON ceramics through aberration-corrected scanning transmission electron microscopy, Scripta Materialia 65 (2011) 656–659.
[7] S.J. Pennycook, *Z*-contrast STEM for materials science, Ultramicroscopy 30 (1989) 58–69.
[8] K. Kimoto, R.J. Xie, Y. Matsui, K. Ishizuka, N. Hirosaki, Direct observation of single dopant atom in light-emitting phosphor of β-SiAlON:Eu^{2+}, Applied Physics Letters 94 (2009) 041908.
[9] H. Yurdakul, S. Turan, Incorporation of the transition metals (Cr and Fe) into β-SiAlON crystal structure, Ceramics International 37 (2011) 1501–1505.
[10] R.G. Duan, G. Roebben, J. Vleugels, O.V.D. Biest, Optimization of microstructure and properties of in situ formed β-O-sialon–TiN composite, Materials Science and Engineering A 427 (2006) 195–202.
[11] B. Bitterlich, S. Bitsch, K. Friederich, SiAlON based cutting tools, Journal of the European Ceramic Society 28 (2008) 989–994.
[12] E. Ayas, A. Kara, H. Mandal, S. Turan, F. Kara, Production of alpha–beta SiAlON–TiN/TiCN composites by gas pressure sintering, Silicates Industriels 69 (2004) 287–292.
[13] Z. Lences, P. Sajgalik, M. Toriyama, M.E. Brito, S. Kanzai, Multifunctional Si_3N_4/(β-SiAlON + TiN) layered composites, Journal of the European Ceramic Society 20 (2000) 347–355.
[14] W. Li, B. Zhang, H. Zhuang, W. Li, Effect of TiN on the corrosion behavior of Y-(α + β)-sialon/TiN materials in hot hydrochloric acidic solutions, Ceramics International 31 (2005) 277–280.
[15] K. Krnel, A. Maglica, T. Kosmac, β-SiAlON/TiN nanocomposites prepared from TiO_2-coated Si_3N_4 powder, Journal of the European Ceramic Society 28 (2008) 953–957.
[16] R.F. Egerton, Electron Energy-Loss Spectroscopy in the Electron Microscope, second edition, Plenum Press, New York, 1996.
[17] D.B. Williams, C.B. Carter, Transmission Electron Microscopy, Spectrometry IV, Plenum Press, New York, 1996.
[18] http://www.webelements.com/atom_sizes.html.
[19] R. Dupree, M.H. Lewis, G. Lengward, D.S. Williams, Co-ordination of Si atoms in silicon–oxynitrides determined by magic-angle-spinning NMR, Journal of Materials Science Letters 4 (1985) 393–395.
[20] R.G. Duan, K.M. Liang, S.R. Gu, The stable energy of glass structure unit, Materials Transactions JIM 39 (1998) 1162–1163.
[21] E.I. Yurieva, A.L. Ivanovskii, Electronic structure of 3D-metal impurities in silicon oxynitride, Journal of Structural Chemistry 42 (2001) 165–171.
[22] I. Tanaka, H. Adachi, Electronic structure of 3d transition elements in β-Si_3N_4, Philosophical Magazine B 72 (1995) 459–473.
[23] R.G. Duan, G. Roebben, C. Sarbu, J. Vleugels, D.V.D. Biest, Microstructural differences in silicon nitrides with and without a small amount of TiN additive, Key Engineering Materials 206–213 (2002) 1181–1184.